Energy Reports 8 (2022) 10533–10545

Contents lists available at ScienceDirect

Energy Reports

journal homepage: www.elsevier.com/locate/egyr

Research paper

Application of the ANOVA method in the optimization of a thermoelectric cooler-based dehumidification system

Mahmoud Eltaweel [a,*], Aya H. Heggy [b], Zaher Mundher Yaseen [c,d,e], Omer A. Alawi [f], Mayadah W. Falah [g], Omar A. Hussein [h], Waqar Ahmed [i], Raad Z. Homod [j], Ali H. Abdelrazek [k]

[a] School of Physics, Engineering and Computer Science, University of Hertfordshire, Hatfield, AL10 9AB, United Kingdom
[b] School of Engineering, London South Bank University, London, United Kingdom
[c] Adjunct Research Fellow, USQ's Advanced Data Analytics Research Group, School of Mathematics Physics and Computing, University of Southern Queensland, QLD 4350, Australia
[d] Department of Earth Sciences and Environment, Faculty of Science and Technology, Universiti Kebangsaan Malaysia, Bangi 43600, Selangor, Malaysia
[e] New era and development in civil engineering research group, Scientific Research Center, Al-Ayen University, Thi-Qar, 64001, Iraq
[f] Department of Thermofluids, School of Mechanical Engineering, Universiti Teknolog Malaysia, 81310 UTM Skudai, Johor Bahru, Malaysia
[g] Building and Construction Engineering Technology Department, AL-Mustaqbal University College, Hillah 51001, Iraq
[h] Department of Mechanical Engineering, College of Engineering-Alsharkat, Tikrit University, Tikrit, Iraq
[i] Takasago i-Kohza, Malaysia-Japan International Institute of Technology, Universiti Teknologi Malaysia, Kuala Lumpur 54100, Malaysia
[j] Department of Oil and Gas Engineering Basrah University for Oil and Gas, Iraq
[k] Department of Mechanical Engineering, University of Malaya, 50603 Kuala Lumpur, Malaysia

ARTICLE INFO

Article history:
Received 21 February 2022
Received in revised form 5 August 2022
Accepted 10 August 2022
Available online xxxx

Keywords:
Dehumidification
Thermoelectric cooler
Analysis of variance
Orientation
Water collection
Optimization

ABSTRACT

In recent studies, Thermo-Electric Coolers (TEC) have been utilized for dehumidification purposes, which is mainly based on the extraction of moisture from humid atmospheric air. The reviewed literature showed that the rate of water collection from the TEC-based system can be affected by various parameters such as the module's input voltage, the heat sink orientation, and tilt angles. In this research, the analysis of variance (ANOVA) was used to examine the significance of these factors and their interaction within the system on the TEC-based dehumidification system. Four levels were investigated for both, the Peltier's input voltage and the rotation angle, and three levels for the tilt angle. This study indicated the significance of the studied factors and their interactions within the dehumidification system along with performing an overall numerical optimization. The experiments were conducted under the same working conditions in an enclosed environment to minimize errors. According to the overall numerical optimization, which was validated experimentally, the optimum system performance was predicted to be obtained at approximately 6.8V Peltier input volt, 65° rotation angle, and 90° tilt angles, with predicted optimum productivities of 0.32278 L/kWh and 13.03 mL/hr. For the same set of parameters, the variation between the experiment and the numerical optimization was less than 4%. The experiments show that when optimizing water collection rates for thermoelectric cooling heat sinks under high humidity conditions, the orientation of the heat sink should be considered.

1. Introduction

Energy management and application with zero emissions and high efficiency are crucial to resolving the energy crisis and environmental deterioration (Su et al., 2017). Because of many advantages, such as compact design, solid-state operation, high reliability, and gas-free emission, thermo-electric cooling (TEC) has become increasingly promising in applications such as battery thermal management systems, space technology, superconductivity, cryogenics, and dehumidification (Jiang et al., 2019). Because humid air is unappealing and can cause common colds, moulds, and skin allergies, humidity control is critical for better comfort conditions. Dehumidifiers can control humidity and prevent a variety of problems (Rafique et al., 2016). Recently, dehu-

* Corresponding author.
E-mail addresses: m.eltaweel@herts.ac.uk (M. Eltaweel), yaseen@alayen.edu.iq (Z.M. Yaseen), omeralawi@utm.my (O.A. Alawi), mayadahwaheed@mustaqbal-college.edu.iq (M.W. Falah), ahmed.waqar@utm.my (W. Ahmed), ali_hassan80@siswa.um.edu.my (A.H. Abdelrazek).

https://doi.org/10.1016/j.egyr.2022.08.193

Nomenclature

T_{amb}	Ambient Temperature
T_h	Surface Temperature of the Hot Side
°C	Degree Celsius
$	US Dollar
A	Ampere
g	Gram
I	Electric Current
K	Kelvin
V	Volt
W	Watt
ΔT	Temperature Difference

Greek Symbols

$(\beta\gamma)_{jk}$	Interaction effect of factors C and B
$(\tau\beta)_{ij}$	Interaction effect of factors A and B
$(\tau\beta\gamma)_{ijk}$	Interaction effect of factors A, B and C
$(\tau\gamma)_{ik}$	Interaction effect of factors A and C
β_j	Effect parameter of factor B (Rotation Angle)
γ_k	Effect parameter of factor C (Tilt Angle)
τ_i	Effect parameter of factor A (TEC Input Volt)

Abbreviations

ANOVA	Analysis of Variance
RH	Relative Humidity
TE	Thermo-Electric
TEC	Thermo-Electric Cooler
TED	Thermo-Electric Dehumidifiers

midifiers have been developed as atmospheric water generators from moist air (Salek et al., 2018). Most dehumidifiers today are refrigerant-based and operate on the vapour compression cycle, which has a significant negative impact on the environment because they use a significant amount of hydrochlorofluorocarbons (HCFCs) or chlorofluorocarbons (CFCs) (Th. Mohammad et al., 2013).

Water generators are another common application of thermoelectric dehumidifiers (Milani et al., 2011). Because of the use of TECs in thermoelectric dehumidifiers (TEDs), it can be used to generate small amounts of portable water from the atmosphere in high-humidity areas. Drinking water scarcity is an unavoidable problem in humid areas, where TED could be used for a variety of purposes (dos Santos et al., 2019). These water generators can be solar-powered and operate as self-contained potable water generators (Bagheri, 2018). TEDs are a category of cooling surface dehumidification without refrigerant. TECs are used in thermoelectric dehumidifiers. It makes use of the TEC's cold surface to condense the moisture in the moist air for water generation or humidity control (Shourideh et al., 2018). Extended surfaces or fins can be used on the cold side surface to improve the heat transfer and allow for a larger surface area for condensation. When the temperature of the finned surface is lower than the saturation temperature of the air in contact with the surface, condensation occurs. Condensation can take place in two ways: as a film or as a drop. The goal of most applications is to have a high heat transfer rate, and dropwise condensation is preferred in this regard since dropwise condensation has high heat transfer rates (Ghajar, 2015). The influence of heat transfer surfaces on wettability (Edalatpour et al., 2018), heat exchanger performance under dehumidification conditions, and surface/droplet interactions, and condensation are all subjects of research (Singh et al., 2019).

The feasibility of using TEC devices for dehumidification was investigated by Milani et al. (2011). It was concluded that the use of a larger surface area of hydrophilic materials could optimize the economic potential. Liu et al. (2017) studied TEC for water generation. The TEC units produced an average of 11.2 g/h with a power consumption of 52.3 W, and the maximum achieved efficiency of the system was 0.215 L/kWh. The use of Peltier elements to generate water for young tree irrigation was investigated by Muñoz García et al. (2013). Because they conducted their experiments in a realistic environment, their maximum relative humidity was 70%. Under these circumstances, the device's efficiency is around 0.1 L/kWh. While Tan and Fok (2013) investigated experimentally the use of TEC for water extraction from the air, the system was able to produce 0.187 L/kWh with 77% relative humidity. Similarly, a maximum efficiency of 0.178 L/kWh was achieved by Joshi et al. (2017). Eslami et al. (2018) presented a thorough thermodynamic analysis of water production using TECs. Their system was capable of producing 26 ml/h of water communing only 20 W of power. They reported production rates ranging from 0.2 to 0.412 L/kWh.

The current study focuses on the influence of the TEC input voltage, rotation angle, and tilt angle on the system water productivity to dehumidify moist air under controlled humidity conditions. The feasibility of using thermoelectric cooling to generate freshwater from the atmosphere or dehumidify has been investigated in several studies. In this study, the analysis of variance (ANOVA) is used to examine the significance of multiple factors and their interactions within the system on the TEC-based dehumidification system and find the optimal parameter combination. To the authors' knowledge, no publications have investigated the effect of rotation angle, tilt angle, and input voltage using analysis of variance for TEC application for atmospheric water generation.

2. Experimental setup and process

2.1. Experimental setup

Two TEC-12715 modules were used that are rated at 15 V, 10 A and were placed inside an insulating foam board. The TEC modules were sandwiched between the heat sink responsible for heat dissipation on the hot side and the condensation surface on the cold side. An Arctic Silver 5 thermal paste is applied between each of the contacting surfaces to ensure good thermal conductivity in the contact areas. Heat is dissipated using a 120 mm long water block heat sink attached to the module's hot side, and water is used as the coolant fluid. A 12 V, 3.6 W pump is used to pump the fluid into the water block and then to a 360 mm computer cooler which consists of 18 flat tubes and is connected to a 200 V AC fan. A plastic plate is used to support the TEC-based system structure to allow the rotation at various angles using an adjustable bolt directly connected to the axial support. The axial support is fixed to a rotating base, making the dehumidification unit tilt at various angles. All the system components, including the dehumidification unit, power supply, and the sensor display screens, are placed on a wooden base, as shown in Fig. 1. Three PT1000 thermocouple sensors were used to measure the temperature of the coolant water, the TEC hot side, and the TEC cold side, as shown in Fig. 2. The sensors have an accuracy of ± 0.5 °C with a range from -50 to 90 °C. The experimental work was conducted indoors, where the temperature and humidity were tested before and after each experiment using a UT333 mini temperature humidity meter. The device has a humidity measuring range of 0∼99%

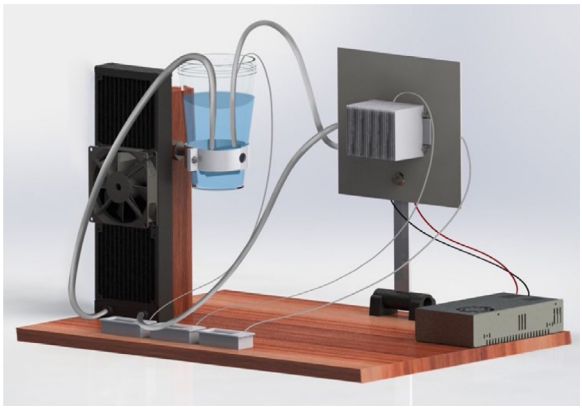

Fig. 1. The experimental setup.

RH and a temperature measuring range of −10∼60 °C, with a maximum inaccuracy of 5%RH and ±1.0 °C, respectively. A 24 V, 240 W power supply was used to supply voltage to the system components with a step-down voltage regulator to adjust the TEC input voltage, depending on the case.

2.2. Experimental design

The experiments' design aims to describe and analyse the variation of different factors under hypothesized conditions that are used to reflect the variation. Accordingly, the interaction between factors during an experiment is also studied.

2.2.1. Cooling system test

The adequacy of heat dissipation from the TEC module's hot side significantly affects the cooling degree on the module's cold side. Accordingly, the first experiment is conducted to examine and select the dehumidification system's optimum cooling method. Four experiments were conducted to show the cooling system's effect on the TEC module's hot and cold temperatures, when a 12 V was supplied to the two TEC modules connected in parallel with a 6 V input for each of them and a 3.35 A current withdrawn. The first experiment was conducted using only the TEC module without any cooling system. The second experiment examined the effect of circulating water through a water cooler block without any other cooling method. In comparison, the third experiment examined adding a water cooler to further cool the water before returning it to the tank. In the final experiment, a fan was attached to the cooler to drive the hot air away and further cool the circulating water. The temperature was recorded in four cases, over 40 min, by taking the readings every minute to ensure the accuracy of measurements.

2.2.2. System performance over time test

It is essential to examine the dehumidification system's performance for a considerable period to determine if the system's results have constant behaviour over time. Hence, this experiment aims to study the dehumidification system's performance over a 12-hour interval to validate the assumption that the system's behaviour can be approximated to be constant over time. Accordingly, this experiment was conducted using the same setup for 12 h, with 12 V supplied to the two TEC modules connected in parallel with 6 V input for each of them and 3.35 A current withdrawn. At the end of the experiment, the amount of water collected from the system was measured using a graduated measuring cup.

Table 1
Design factors and their levels.

Levels	Factors		
	A TEC input voltage	B Rotation angle	C Tilt angle
1	6 V	0°	0°
2	8 V	30°	45°
3	10 V	60°	90°
4	12 V	90°	

2.2.3. TEC system parametric study

The analysis of variance is a valuable tool for examining the significance of various variables of interest on the required response (Bertinetto et al., 2020). In this study, ANOVA is used to examine the significance of multiple factors and their interaction within the system on the TEC-based dehumidification system. The system responses are selected primarily to simulate the interaction and quadratic effects of the system parameters on the reaction surface. Furthermore, they are utilized to discover system strengths and weaknesses and to find the ideal settings for the system (Bertinetto et al., 2020). In this model, the amount of water collected per kilowatt-hour (L/kWh) was chosen as the response.

Any experiment benefits from the replication principle because it produces more accurate results and helps the investigator determine the actual mean response. In addition, this experimental design would help determine the value of the interventions or the ANOVA's validity because it can provide precise measures. One of the most critical issues in experimental design is correctly calculating the high power and risk of failure. Three replicates were used in this research. An approximation of the standard deviation is used to interpret the output response data. In order to measure variation, predictability, and error, the standard deviation is calculated by comparing the change in the output with the change in the input and output (Jankovic et al., 2021). Following that, an analysis is conducted, and the test's power is determined by utilizing design expert software's capabilities.

2.2.3.1. Selection of factors. A comprehensive literature survey was conducted previously, highlighting the factors that need to be examined in a dehumidification system. The chosen factors are the TEC input voltage, rotation angle, and tilt angle of the condensation surface. The voltage input to the TEC module is crucial for module function because it impacts the temperature gradient formed across the module's connections (Jankovic et al., 2021). According to Hand and Peuker (2019), the thermoelectric cooling heat sink orientation has a significant effect on the rate of water condensation in a dehumidification system. Thus, in this study, the rotation angle and tilt angle of the cold side heat sink were chosen as design factors that needed to be studied.

The chosen design factors and their levels are illustrated in Table 1. The input volt to the TEC is varied within four levels, ranging from 6 V to 12 V with an increment of 2 V. The second factor represents the dehumidification unit's rotation angle, which is varied into four angles, as shown in Fig. 3. while the tilt angle is studied at three different levels, as shown in Fig. 4.

One of the two popular ANOVA approaches is based on the factorial technique employed when performing tests with a multitude of variables and stages of research (Jankovic et al., 2021). The analysis conducted in this study involved using factorial analysis to evaluate the three components' influences on the answers at different levels. This experiment features a four-level factorial design, with A and B running concurrently with three C levels. This type of test is often used to evaluate the relative importance of elements and their interactions. For example, the

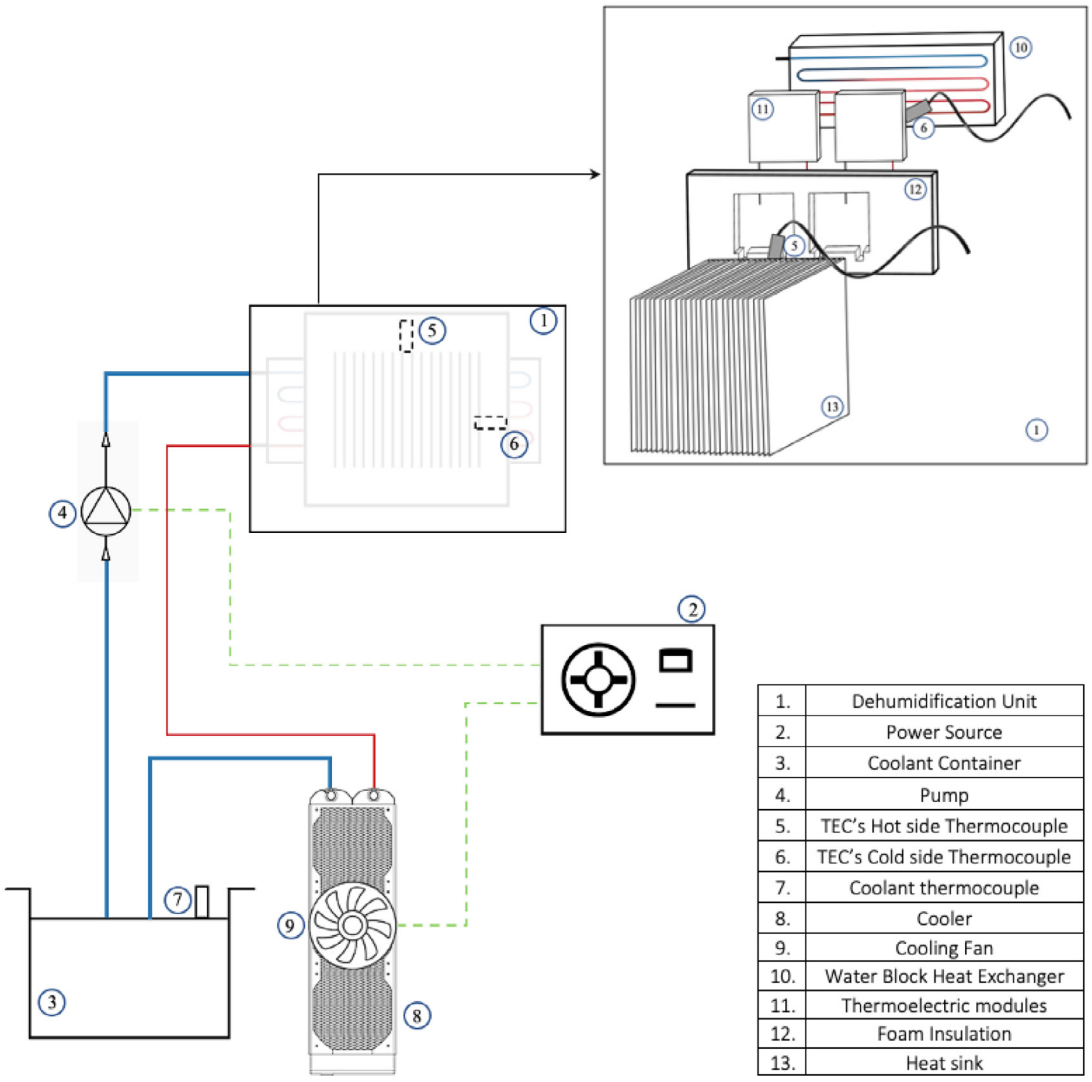

Fig. 2. The schematic diagram of the used setup.

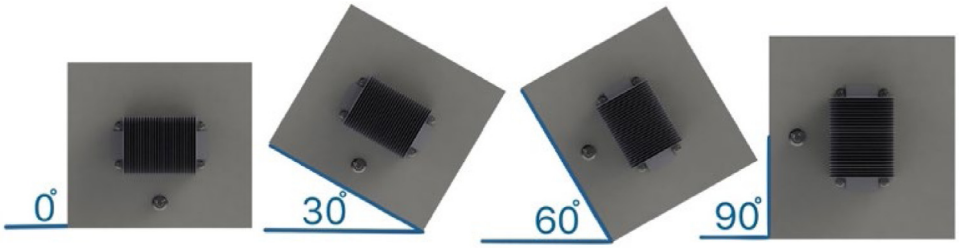

Fig. 3. Schematic diagram for the rotation angles of the dehumidification unit.

null hypothesis suggests that the total mean for all treatments is equal, suggesting that there is no variation in treatment means. In contrast, the alternate hypothesis predicts that at least one therapy will significantly differ on average. The hypotheses presented here are the null and alternative hypotheses for each treatment, while the last four hypotheses detail the null and alternative hypotheses for treatment interaction.

$$H_o : \tau_i = 0 \; vs. \; H_1 : at \; least \; one \; \tau_i \neq 0$$
$$H_o : \beta_j = 0 \; vs. \; H_1 : at \; least \; one \; \beta_j \neq 0$$
$$H_o : \gamma_k = 0 \; vs. \; H_1 : at \; least \; one \; \gamma_k \neq 0$$
$$H_o : (\tau\beta)_{ij} = 0 \; vs. \; H_1 : at \; least \; one \; (\tau\beta)_{ij} \neq 0$$
$$H_o : (\tau\gamma)_{ik} = 0 \; vs. \; H_1 : at \; least \; one \; (\tau\gamma)_{ik} \neq 0$$
$$H_o : (\beta\gamma)_{jk} = 0 \; vs. \; H_1 : at \; least \; one \; (\beta\gamma)_{jk} \neq 0$$
$$H_o : (\tau\beta\gamma)_{ijk} = 0 \; vs. \; H_1 : at \; least \; one \; (\tau\beta\gamma)_{ijk} \neq 0$$

where τ_i is the effect parameter of factor A (TEC Input Volt), β_j is the effect parameter of factor B (Rotation Angle), γ_k is the effect parameter of factor C (Tilt Angle), $(\tau\beta)_{ij}$ is the interaction effect of factor A & B, $(\tau\gamma)_{ik}$ is the interaction effect of factor A & C, $(\beta\gamma)_{jk}$ is the interaction effect of factor B & C, and $(\tau\beta\gamma)_{ijk}$ is the interaction effect of factor A, B & C. In these experiments,

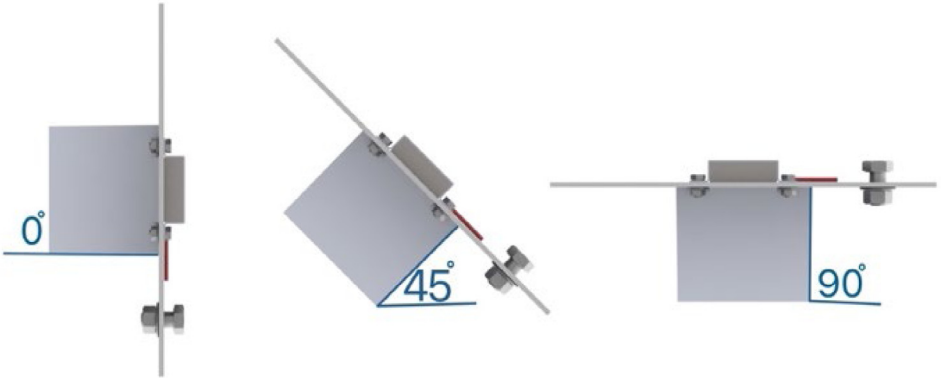

Fig. 4. Schematic diagram for the tilt angles of the dehumidification unit.

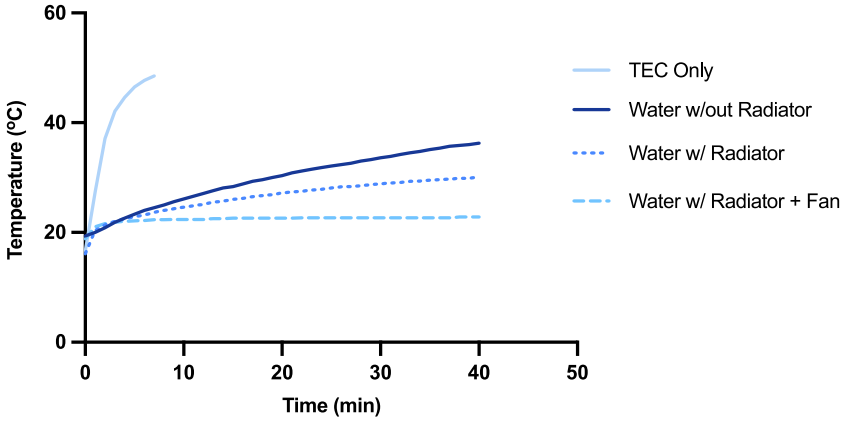

Fig. 5. The influence of cooling system on the hot side temperature of the TEC.

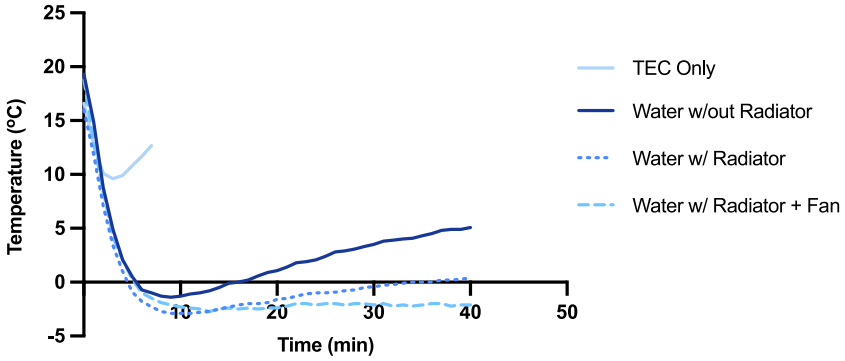

Fig. 6. The influence of cooling system on the cold side temperature of the TEC.

the system's performance was analysed based on the amount of water collected for each case. The experiment duration for each case was 30 min, and water was left to drain for another 10 min before being measured.

3. Results and discussion

3.1. Cooling system test

The cooling system's influence on the hot and cold side temperatures of the TEC module was observed. Fig. 5 illustrates the module's hot side temperature over 40 min when different cooling techniques were used. It can be observed that when no cooling system was used and the TEC was working independently, the hot side temperature of the module increased rapidly over a short time. This indicated the need for an adequate cooling system to be installed in the system to dissipate the heat generated on the module's hot side. Three different scenarios were then studied. The first one is based on using only coolant water that flows through the water block attached to the TEC's hot side without any additional techniques. In the second cooling technique, a cooler was installed in the system, through which the water flows before returning to the tank. Finally, a fan was attached to the cooler to cool the flowing water further by driving the hot air away from the cooler. The hot side temperature is highly affected by the amount of heat dissipated in each cooling system, and the addition of a fan to the cooler resulted in the most stable temperature. The hot side temperature's constant behaviour in the last case shows that this system can dissipate all the heat added to it.

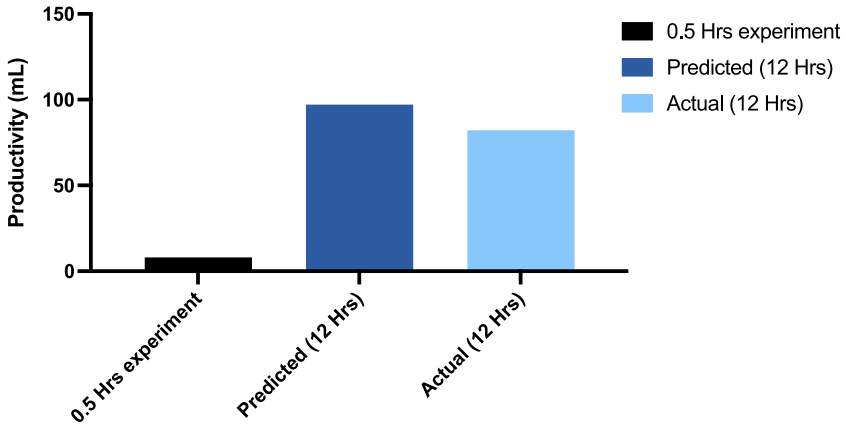

Fig. 7. The predicted vs. actual amount of water collected from the system after 12 h.

Fig. 8. Ice formation on the heat sink during the 12 h experiment.

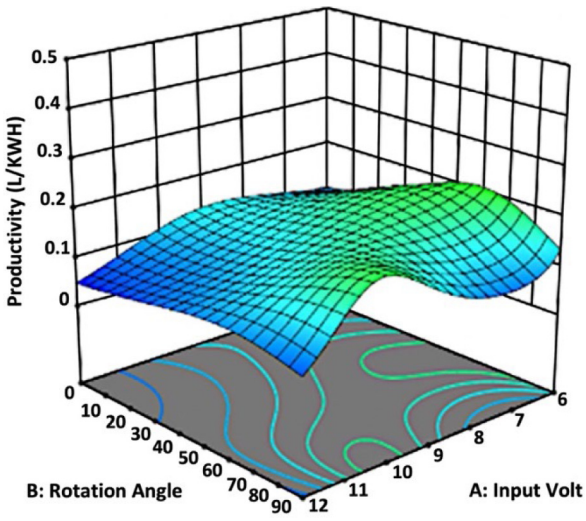

Fig. 9. 3D surface plot for the productivity at 0° tilt angle.

On the other hand, Fig. 6 illustrates the dependency of the TEC module's cold side temperature on its hot side temperature. The figure showed that the cold temperature decreases until it reaches a certain point for all the studied cases, after which the temperature starts to increase again. In a dehumidification process, achieving the lowest possible temperature is the main target to harvest moisture from the air, even for low dew point temperatures. The lowest temperature was always achieved by the cooling technique with the cooler and the fan. This shows the dependency of the module's cold side temperature on the amount of heat dissipated from its hot side. Accordingly, using the proper cooling system can allow the condensation surface to achieve low temperatures capable of harvesting more water from the air. Thus, the cooling system with the cooler and fan was selected and used in the remaining studies to ensure the consistency of the temperatures on the two sides of the TEC module.

3.2. System performance over time

In this experiment, the TEC-based dehumidification system's performance over 12 h was observed to validate the assumption that the system has approximately constant behaviour over time. 6 V was supplied to each TEC module, and a cooler with a fan cooling technique was used to dissipate the heat from the hot side of the module. First, the experiment was conducted on a 30-minute interval, and the amount of water was recorded and used to estimate a predicted value for the amount of water collected after 12 h. It was found that over 12 h, the system is predicted to harvest 97.2 mL. However, after experimenting for 12 h using the same conditions, it was found that the actual amount of water collected in 12 h is 82.2 mL, which was lower than the predicted value (see Fig. 7).

As illustrated in Fig. 8, during the 12-hour interval, the heat sink was completely covered in ice. The lower amount of water collection could be attributed to the accumulation of ice on the metallic fins, resulting in a complete block of ice; thus, lower surface area is subjected to moist air which result in harvesting lower amount of water than expected.

Table 2
ANOVA results for the dehumidification system's productivity (L/kWh).

Source	Sum of squares	df	Mean square	F-value	p-value	Significance
Model	59.22	36	1.65	45.76	<0.0001	Significant
A-Input volt	0.9388	1	0.9388	26.11	<0.0001	Significant
B-Rotation angle	0.0077	1	0.0077	0.2134	0.6451	Not significant
C-Tilt angle	0.5286	1	0.5286	14.70	0.0002	Significant
AB	0.5906	1	0.5906	16.43	<0.0001	Significant
AC	0.0174	1	0.0174	0.4844	0.4880	Not significant
BC	0.0330	1	0.0330	0.9172	0.3404	Not significant
ABC	0.9534	1	0.9534	26.52	<0.0001	Significant
Residual	3.74	104	0.0360			
Lack of fit	0.5940	11	0.0540	1.60	0.1124	Not significant
Pure error	3.14	93	0.0338			
Cor total	62.96	140				

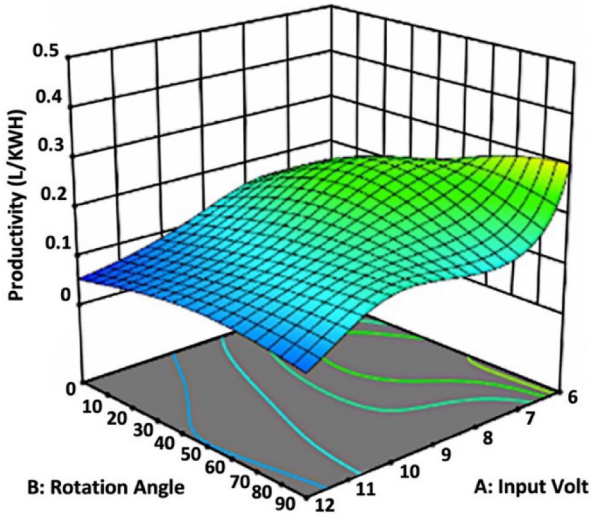

Fig. 10. 3D surface plot for the productivity at 45° tilt angle.

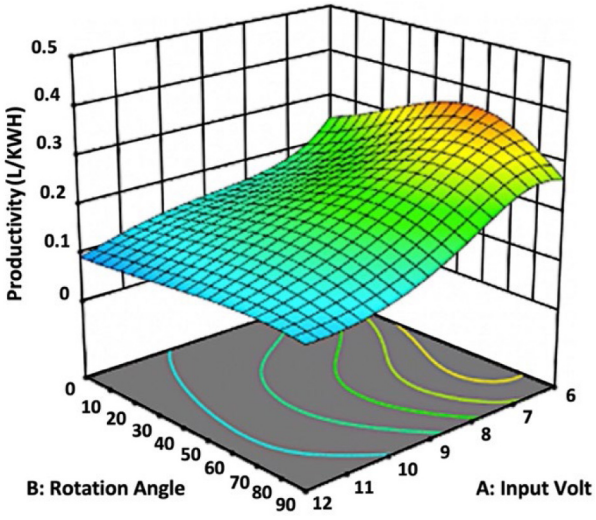

Fig. 11. 3D surface plot for the productivity at 90° tilt angle.

3.3. TEC system parameters

System working parameters such as the TEC input volt and condensation surface's rotation and tilt angles are studied and analysed using the analysis of variance approach. In this analysis, system productivity was chosen as the response to evaluate the dehumidification system's working parameters. An analysis of variance was conducted, and the results of the main factors and their interactions were tabulated for productivity (L/kWh) (See Table 2).

To establish the significance of each factor and its mean variation, F-values are calculated for each factor and its interactions, as well as for the lack of fit. Following that, the relevant P-values are calculated with a 95% confidence interval. All terms are significant, with a *p*-value less than 0.05, except for the rotation angle, the interaction between the tilt angle with the input volt and the tilt angle with the rotation angle, which all have a *p*-value greater than 0.05, demonstrating the term's insignificance. The conclusions based on this analysis indicate that the effect of rotation angle on the system's productivity does not have a significant effect. In addition, the interaction of the tilt angle with the rotation angle and TEC's input volt is not significant and could be neglected. In line with the results reported in the ANOVA table, the lack of fit has an F-value of 1.6, which suggests that there is no significant lack of fit. These findings demonstrate that the proposed model accurately depicts the dataset.

3.3.1. Fit statistics

In regression models, the relationship between input variables and dependent responses is described using a mathematical model. To further highlight the information from the Design-Expert software. Regression analysis indicates that the coefficient of determination (R^2) is 0.9406, with very few data points separating the regression line and the response points. According to the adjusted R^2, which considers the useless and valuable parameters in the model, the variability in the model was represented. The adjusted R^2 value is 0.901, which means that just a minor variance percentage occurred. To state the model's capacity to forecast new observations, one may look at the predicted R^2. Applying the table result shows that the difference between the R^2 adjusted and predicted is 0.2, suggesting a reasonable correlation. Whereas acceptable precision evaluates the signal-to-noise ratio of the data, inadequate precision measures noise only. This means that a sufficient signal was acquired with a satisfactory precision ratio of 29.76.

3.3.2. Plots

The productivity (L/kWh) of a TEC-based dehumidification system has been investigated using three factors that have been identified as the main influencing factors in the literature. Two of those factors are related to the rotation and tilt angles of the condensation heat sink, while the third is the TEC input volt.

The surface plots for the three tested tilt angles (see Figs. 9–11) show that regardless of the input volt, peak productivity occurs at rotation angles ranging from 60° to 90°. Thus, as shown in Fig. 12(a), a rotation angle of 90° causes droplet accumulation and bridging, resulting in low productivity, whereas a rotation angle of less than 60° reduces productivity due to the high surface tension between the water and the heat sink fins, as shown in

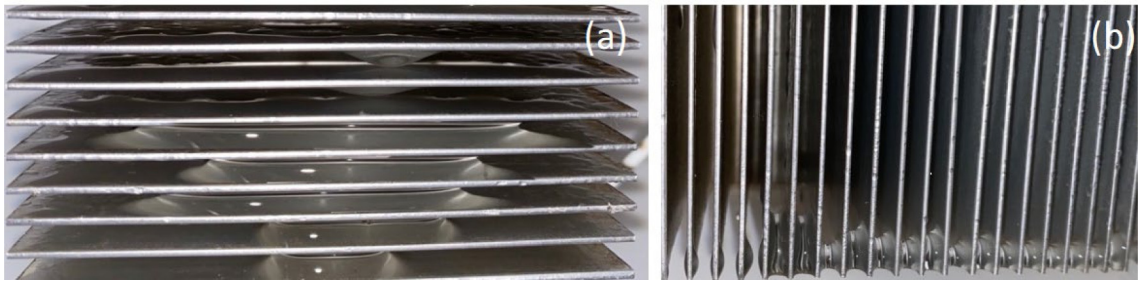

Fig. 12. (a) Droplet accumulation and bridging at 90° rotation angle, (b) High surface tension and droplets' bridging at 0° rotation angle.

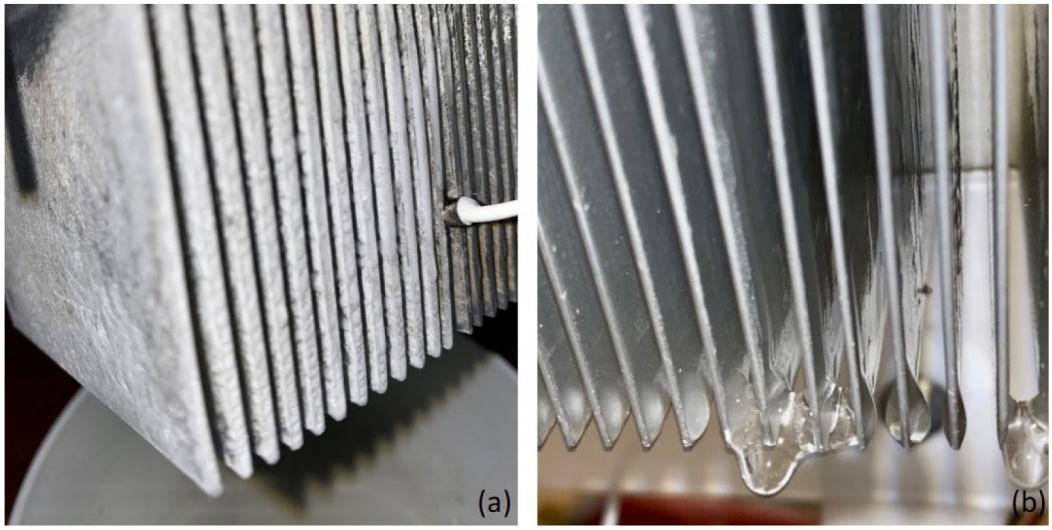

Fig. 13. The heat sink under the same rotation angle and tilt angle for, (a) 12 V input volt, and (b) 10 V input volt.

Fig. 12(b). Water droplets overcome high surface tension and are easily removed from the surface at rotation angles greater than 60° and less than 90°, resulting in high productivity.

According to the studied parameter of water production based on the amount of water collected per kilowatt-hour, increasing the input volt will result in higher electricity usage, but if the production of water is significantly improved by increasing the input volt, the productivity will be high. The lowest studied input volt produced a good amount of water while using a low amount of electricity, whereas the input volt of 8 V produced more water than 6 V but the difference was not significant in terms of water amount, making the amount produced per KWh low. 12 V input volt have the least amount of productivity regardless of the rotation angle or the tilt angle of the heat sink. The TEC cold side temperature decreases as the input voltage increases, implying that the input voltage of 12 V resulted in the lowest surface temperature of the heat sink. However, at 12 V, the heat sink temperature was in the frost point causing the water vapour to freeze on the heat sink's surface, as shown in Fig. 13(a), reducing the surface area for condensation and influencing water production. The surface temperature, on the other hand, was in the dew point without an effect on water production at 10 V, as shown in Fig. 13(b).

As shown in Figs. 9, 10, and 11, the lowest productivities were obtained at the highest TEC input volt for all tilt angles, regardless of rotation angle. This is due to the high TEC electricity consumption, which is not proportional to the amount of water produced, as a result of water freezing on the heat sink surface, affecting system productivity and causing the input volt rise to have a sinusoidal response for water productivity.

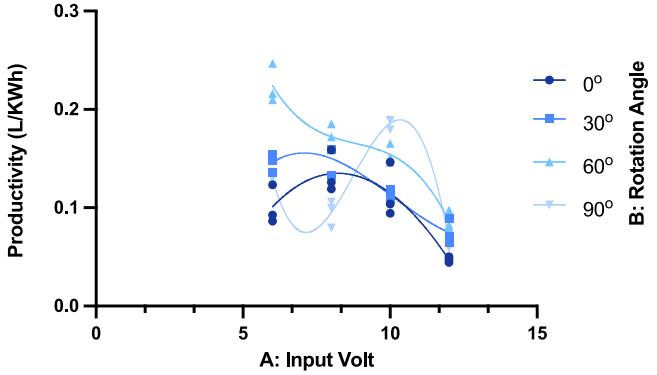

Fig. 14. 2D interaction plot for the productivity between the input volts and rotation angles at 0° tilt angle.

Figs. 14, 15, and 16 depict the relationship between input volt and productivity for the four rotation angles tested. For all tilt and rotation angles, increasing the input volt reduces productivity. The relationship between the three studied parameters is more complicated, which means that in certain situations, the productivity was higher at higher input volt, as shown in Fig. 14 for rotation angle of 60°, where input volt of 10 V have the highest productivity, which can be attributed to the ease with which water droplets leave the heat sink surface with a tilt angle of 0°.

The increase in tilt angle improves productivity because the surface tension between water droplets and the heat sink is high at 0° tilt angle, and water bridging can be observed, as

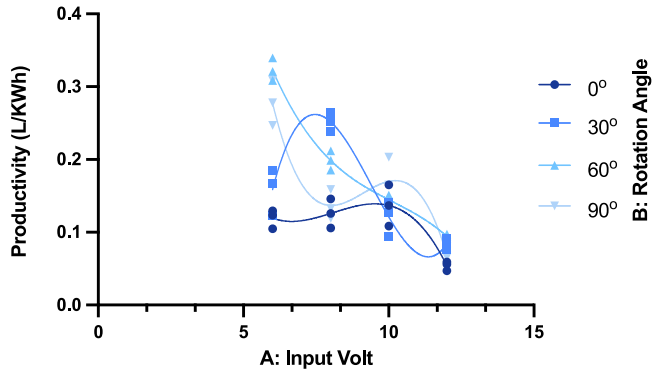

Fig. 15. 2D interaction plot for the productivity between the input volts and rotation angles at 45° tilt angle.

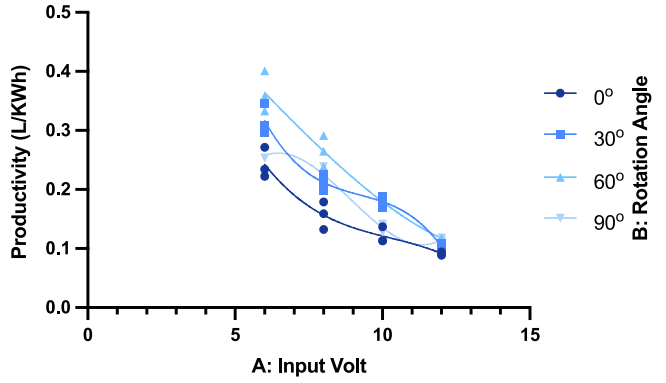

Fig. 16. 2D interaction plot for the productivity between the input volts and rotation angles at 90° tilt angle.

shown in Fig. 17(a), whereas at higher tilt angles, the droplets can overcome the surface tension and there is less bridging, as shown in Fig. 17(b). The highest productivities were obtained at 6 V and 30° and 60° rotation angles when the heat sink was tilted 45°, as shown in Fig. 15. Fig. 16, where the tilt angle is 90°, helps the water droplets leave the heat sink surface faster, resulting in the highest productivity at the lowest input volt and decreasing productivity as the input volt increases. However, the 90° tilt angle combined with the 90° rotation angle reduced productivity due to water bridging.

Fig. 18 represents the water production in terms of amount of water produced per hour for the three tested tilt angles. The rise in the tilt angle increases the average water production, with a tilt angle of 90° producing the most water. The rotation angle of the heat sink affects water production, with a rotation angle of 60° producing the most water for all tested input voltages, and tilt angles. The effect of increasing the input volt improve the water production, expect for 12 V were the surface temperature was below the dew point, as shown in Fig. 12(a). In addition, the tilt angle of 0° has the lowest productivity in all the cases except for the rotation angle of 60°, where it shows high variability in the productivity as the input voltage increases, with maximum productivity at 10 V. The low productivity at 0° tilt angle can be attributed to the high surface tension between the droplets and the surfaces of the fins, which aggravates droplet separation from the surface until their weight overcomes this tension, as illustrated in Fig. 18. The droplets bridging at higher tilt angles, on the other hand, cannot be sustained for long and tend to leave the surface more easily, allowing more water to condense on the cleared surface. The rise in the rotation angle also increases the water production significantly until it reaches 90°, at which point water bridging becomes an issue.

Figs. 19, 20, 21, and 22 show the relationship between input voltage and productivity at various tilt angles for rotation angles of 0°, 30°, 60°, and 90°, respectively. By increasing Peltier's input volt and decreasing the tilt angle, productivity tends to decrease. The tilt angle of 90° achieves the highest consistent productivity over different voltage inputs for all tilt rotation angles, while the tilt angle of 45° achieves the highest productivity for the rotation angle of 90°, as shown in Fig. 22. This is due to the beneficial flow pattern and the increased convection between the fin surface and the surrounding air. Furthermore, higher tilt angles do not allow droplets to bridge for an extended period of time; as a result, they tend to leave the surface more quickly, allowing more water to condense on the cleared surface. The productivity of the dehumidification system is lowest at 0° rotation angle due to a less beneficial flow pattern within the fins than at other higher rotation angles. Furthermore, regardless of tilt or rotation angle, as input voltage increases, the system's productivity decreases, with little variation between results at different rotation angles.

Figs. 23, 24, 25, and 26 show how the rotation and tilt angles affect productivity at 6 V, 8 V, 10 V, and 12 V input volts to the Peltier modules, respectively. At all input volts, the rotation angle and productivity have an exponential relationship. In all cases, increasing the tilt angle increases productivity; however, increasing the rotation angle increases productivity to a point after which it begins to decline. The rotation angle has no effect on the productivity trend for an input voltage of 12 V and a tilt angle of 90°; however, if the rotation angle is increased beyond the tested values, productivity will be reduced. The highest average productivity was obtained for a 90° tilt angle at the four tested input volts. This is due to the fact that the increased density of the air may have a beneficial effect when the fins are oriented vertically, as oversaturated air sinks relative to typical ambient air. The heavier air that falls out of the heat sink is moved across the fin surface by an angled fin. The longer air is allowed to contact the fin surface, the more likely condensation will form.

Furthermore, increasing the rotation angle to 90° results in relatively high productivity. However, due to droplet accumulation over time and extreme bridging, almost all of the water collected was drained from the heat sink at the end of the test, as shown in Fig. 12(a). Thus, the 90° rotation angle is extremely inefficient over time because the system would constantly require droplet removal to maintain the system's high output. According to this study, reaching capacity or engaging in excessive bridging has a negative impact on the collection rate.

3.3.3. Optimization

A numerical optimization between the system's responses was conducted using Design-Expert software. Results indicated that optimum system performance would be obtained at approximately 6.8 V TEC input volt, 65° rotation angle, and 90° tilt angle as shown in Fig. 27. This parameter combination would result in the optimum system's productivity in terms of litres produced per kilowatt-hour used and the litres produced per hour of the system's operation at maximum desirability of 0.915. Fig. 28, on the other hand, illustrates a more visualized optimization using contour graphs. The red regions demonstrate the optimum regions for the system's response with the predicted optimum productivity of 0.32278 L/kWh. The numerical optimization results were validated by running an experiment at the software's suggested levels of 6.8 V TEC input volt, 65° rotation angle, and 90° tilt angle. The experiment was repeated three times, and the system's average productivity over the three trials was 0.33419 L/kWh. For the same set of parameters, the variation between experiments and software was less than 4%.

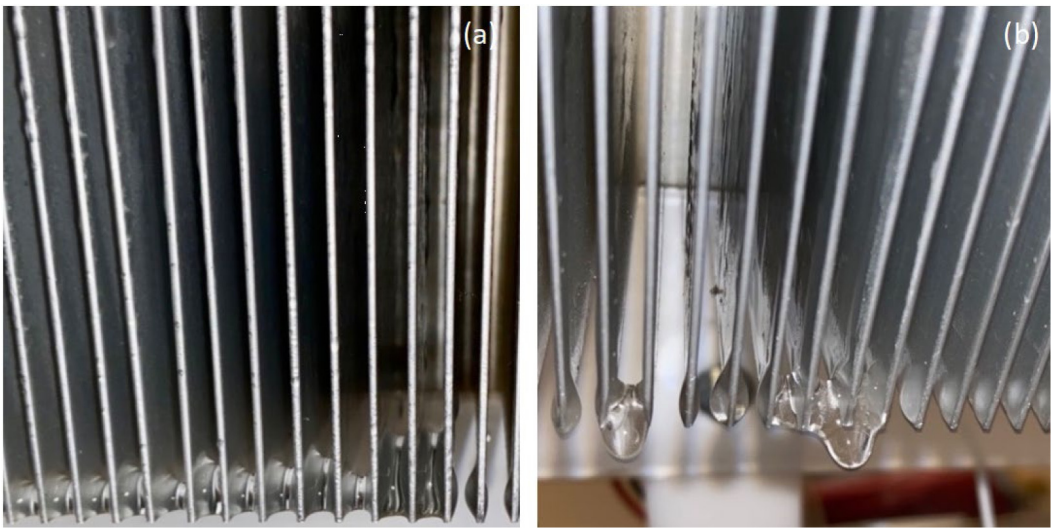

Fig. 17. (a) High surface tension and droplets' bridging at 0° tilt angle, (b) Droplets overcoming surface tension and less bridging at higher tilt angles.

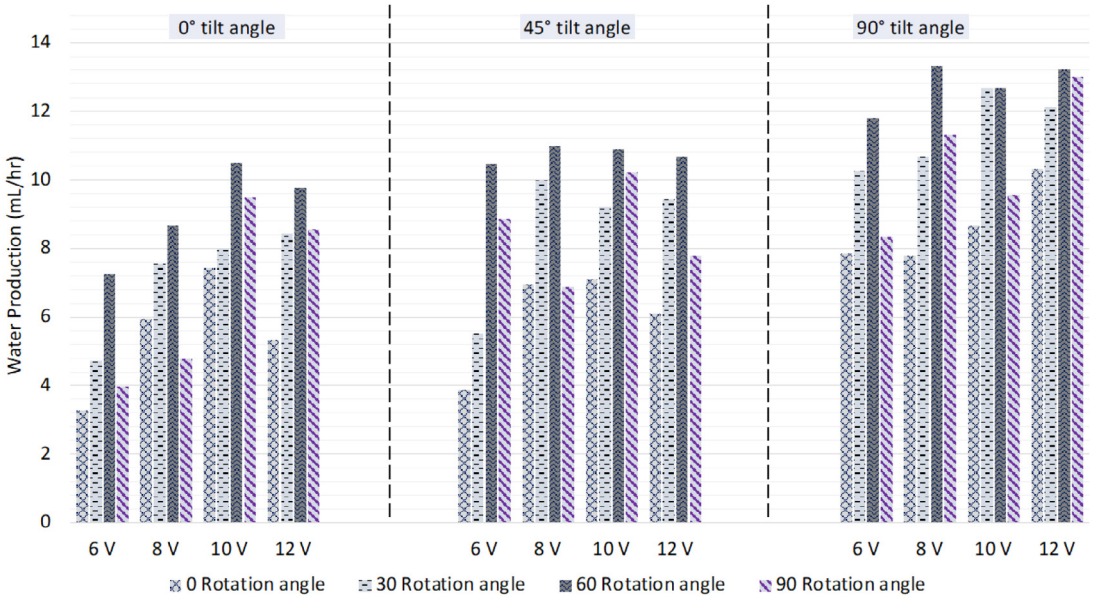

Fig. 18. The water production rate per hour for the three tested tilt angles.

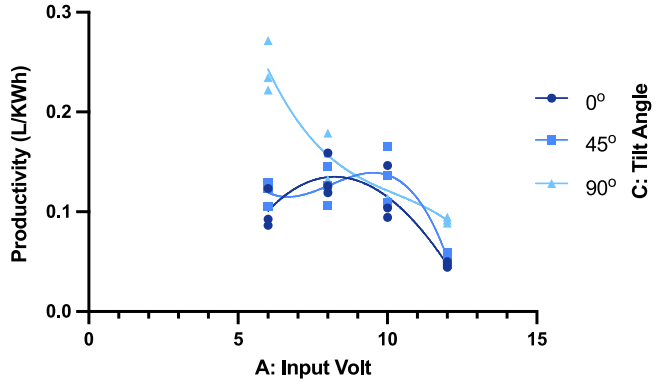

Fig. 19. 2D interaction plot for the productivity between input volts and tilt angles at 0° rotation angle.

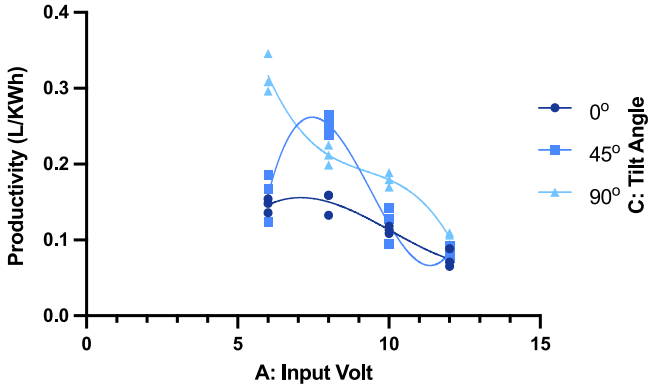

Fig. 20. 2D interaction plot for the productivity between input volts and tilt angles at 30° rotation angle.

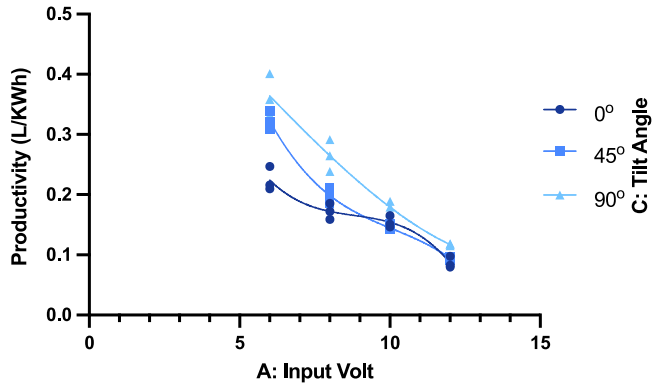

Fig. 21. 2D interaction plot for the productivity between input volts and tilt angles at 60° rotation angle.

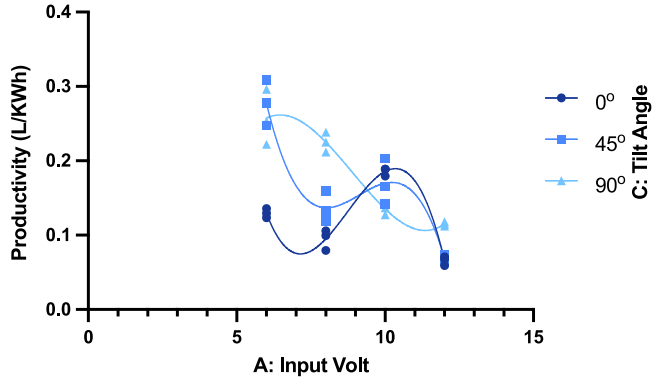

Fig. 22. 2D interaction plot for the productivity between input volts and tilt angles at 90° rotation angle.

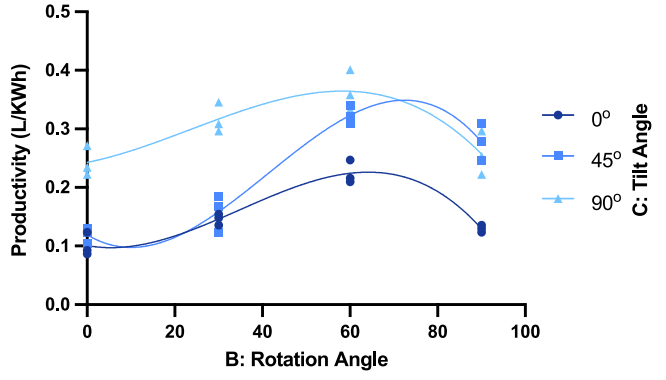

Fig. 23. 2D interaction plot for the productivity between rotation angles and tilt angles at 6 V input volt.

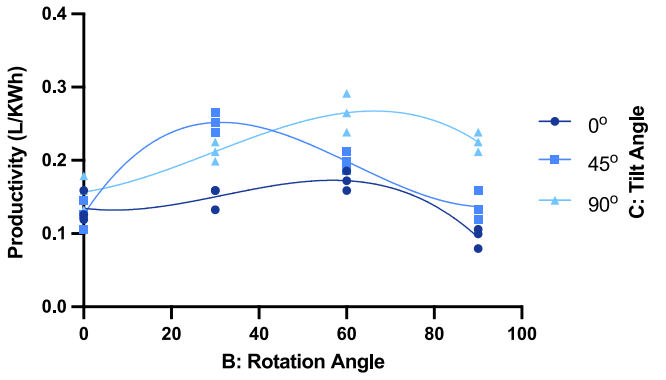

Fig. 24. 2D interaction plot for the productivity between rotation angles and tilt angles at 8 V input volt.

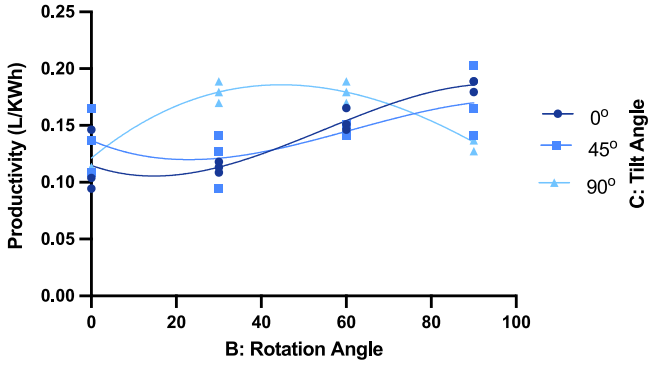

Fig. 25. 2D interaction plot for the productivity between rotation angles and tilt angles at 10 V input volt.

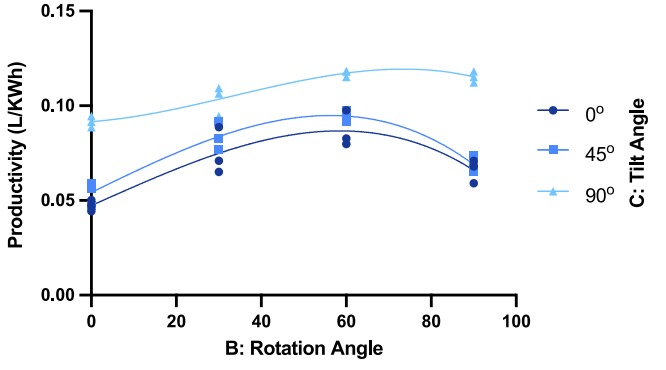

Fig. 26. 2D interaction plot for the productivity between rotation angles and tilt angles at 12 V input volt.

4. Conclusion

The analysis of variance (ANOVA) method is proposed for analysing the TEC's performance and determining the optimal factors that correspond to the system's maximum productivity in terms of the amount of water collected per kilowatt-hour (L/kWh). An investigation of the cooling techniques for the TEC's hot side was conducted in order to select the most appropriate cooling technique to maintain the temperature of the TEC and to be used throughout the experimental work. The use of a cooler with a fan produced the most stable temperature, which was then used to investigate the performance of the TEC over 12 h in order to validate the assumption that the system has roughly constant behaviour over time. Due to ice formation on the fins, which resulted in a lower surface area for dehumidification, the predicted value of the TEC's productivity to be collected after 12 h was 15% lower than the actual value. In this study, the ANOVA method is used to determine the optimal parameters and assess the impact of the chosen parameters on performance. The ANOVA analysis was performed on three variables: Peltier's input volt, rotation angle, and tilt angle. The Peltier's input volt was varied in four levels, from 6 V to 12 V with a 2 V increment, and the rotation angle was varied from 0° to 90° with a 30° increment. Furthermore, the tilt angle was investigated at three different levels: 0°, 45°, and 90°. The significance of the investigated factors and their interactions within the dehumidification system was demonstrated in this study. Peak productivity occurs between rotation angles

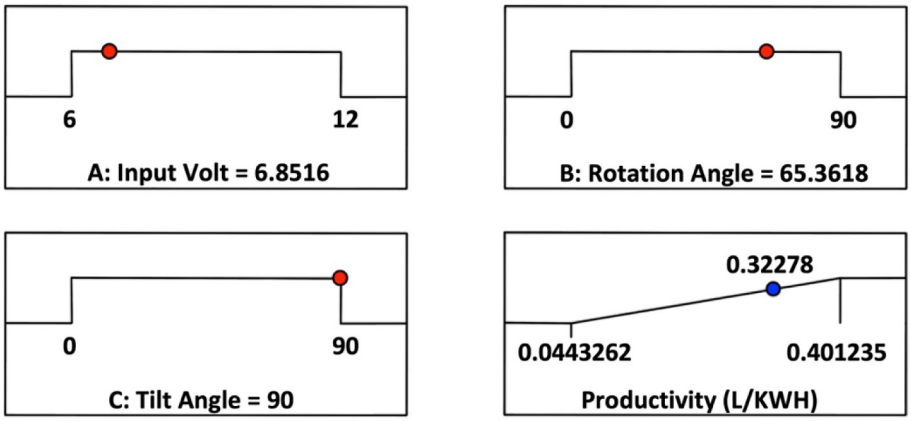

Fig. 27. Numerical optimization for productivity (L/kWh).

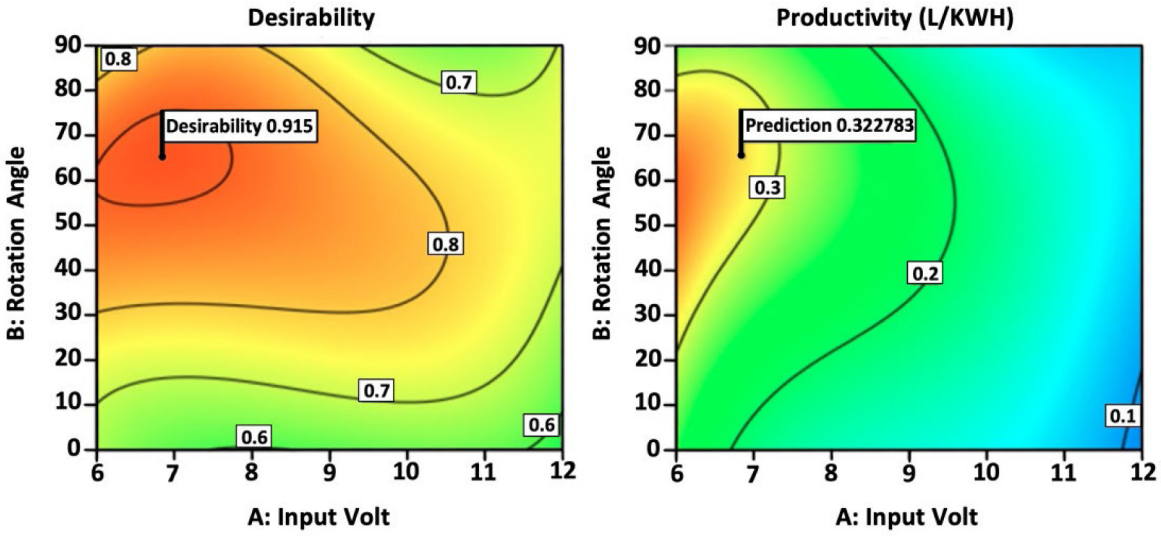

Fig. 28. Optimization contour of the productivity (L/kWh).

of 60° and 90°. A rotation angle of 90 degrees causes droplet accumulation and bridging, resulting in low productivity, whereas a rotation angle of less than 60 degrees reduces productivity due to the high surface tension between the water and the heat sink fins. The heat sink temperature was nearing the frost point at 12 V, causing water vapour to freeze on the heat sink's surface, reducing the surface area for condensation and influencing water production. The overall numerical optimization revealed that the best system performance would be obtained at approximately 6.8 V Peltier input volt, 65° rotation angle, and 90° tilt angles, with predicted optimum productivities of 0.32278 L/kWh and 13.03 mL/h. The difference between experimental validation and numerical optimization for the same set of parameters was less than 4%.

CRediT authorship contribution statement

Mahmoud Eltaweel: Conceptualization, Methodology, Formal analysis, Writing – original draft. **Aya H. Heggy:** Validation, Writing – review & editing, Visualization. **Zaher Mundher Yaseen:** Supervision, Writing – original draft. **Omer A. Alawi:** Investigation, Software. **Mayadah W. Falah:** Methodology, Writing – review & editing. **Omar A. Hussein:** Formal analysis, Investigation. **Waqar Ahmed:** Writing - review & editing. **Raad Z. Homod:** Writing - review & editing. **Ali H. Abdelrazek:** Writing - review & editing.

Declaration of competing interest

The authors declare that they have no known competing financial interests or personal relationships that could have appeared to influence the work reported in this paper.

Data availability

Data will be made available on request.

Acknowledgements

The authors would like to thank Dr. Hussein Togun and Balaji Bakthavatchalam for checking the technicality of the paper and the language revision/edits. In addition, the authors would like to thank Al-Mustaqbal University College for providing technical support for this research.

References

Bagheri, F., 2018. Performance investigation of atmospheric water harvesting systems. Water Resour. Ind. 20, 23–28. http://dx.doi.org/10.1016/j.wri.2018.08.001.

Bertinetto, C., Engel, J., Jansen, J., 2020. ANOVA simultaneous component analysis: A tutorial review. Anal. Chim. Acta X 6, 100061. http://dx.doi.org/10.1016/j.acax.2020.100061.

dos Santos, S.M., Silva, J.F.F., dos Santos, G.C., de Macedo, P.M.T., Gavazza, S., 2019. Integrating conventional and green roofs for mitigating thermal discomfort and water scarcity in urban areas. J. Clean. Prod. 219, 639–648. http://dx.doi.org/10.1016/j.jclepro.2019.01.068.

Edalatpour, M., Liu, L., Jacobi, A.M., Eid, K.F., Sommers, A.D., 2018. Managing water on heat transfer surfaces: A critical review of techniques to modify surface wettability for applications with condensation or evaporation. Appl. Energy 222, 967–992. http://dx.doi.org/10.1016/j.apenergy.2018.03.178.

Eslami, M., Tajeddini, F., Etaati, N., 2018. Thermal analysis and optimization of a system for water harvesting from humid air using thermoelectric coolers. Energy Convers. Manage. 174, 417–429. http://dx.doi.org/10.1016/j.enconman.2018.08.045.

Muñoz García, M.A., Moreda, G.P., Raga-Arroyo, M.P., Marín-González, O., 2013. Water harvesting for young trees using peltier modules powered by photovoltaic solar energy. Comput. Electron. Agric. 93, 60–67. http://dx.doi.org/10.1016/j.compag.2013.01.014.

Ghajar, A.J., 2015. Heat and Mass Transfer. McGraw-Hill.

Hand, C.T., Peuker, S., 2019. An experimental study of the influence of orientation on water condensation of a thermoelectric cooling heatsink. Heliyon 5 (10), e02752.

Jankovic, A., Chaudhary, G., Goia, F., 2021. Designing the design of experiments (DOE) – An investigation on the influence of different factorial designs on the characterization of complex systems. Energy Build. 250, 111298. http://dx.doi.org/10.1016/j.enbuild.2021.111298.

Jiang, L., Zhang, H., Li, J., Xia, P., 2019. Thermal performance of a cylindrical battery module impregnated with PCM composite based on thermoelectric cooling. Energy 188, 116048. http://dx.doi.org/10.1016/j.energy.2019.116048.

Joshi, V.P., Joshi, V.S., Kothari, H.A., Mahajan, M.D., Chaudhari, M.B., Sant, K.D., 2017. Experimental investigations on a portable fresh water generator using a thermoelectric cooler. In: Int. Conf. Recent Adv. Air Cond. Refrig. RAAR 2016 10-12 Novemb. 2016 Bhubaneswar India, Vol. 109. pp. 161–166. http://dx.doi.org/10.1016/j.egypro.2017.03.085.

Liu, S., et al., 2017. Experimental analysis of a portable atmospheric water generator by thermoelectric cooling method. In: Proc. 9th Int. Conf. Appl. Energy, Vol. 142. pp. 1609–1614. http://dx.doi.org/10.1016/j.egypro.2017.12.538.

Milani, D., Abbas, A., Vassallo, A., Chiesa, M., Bakri, D.A., 2011. Evaluation of using thermoelectric coolers in a dehumidification system to generate freshwater from ambient air. Chem. Eng. Sci. 66 (12), 2491–2501. http://dx.doi.org/10.1016/j.ces.2011.02.018.

Rafique, M.M., Gandhidasan, P., Bahaidarah, H.M.S., 2016. Liquid desiccant materials and dehumidifiers – A review. Renew. Sustain. Energy Rev. 56, 179–195. http://dx.doi.org/10.1016/j.rser.2015.11.061.

Salek, F., Moghaddam, A.N., Naserian, M.M., 2018. Thermodynamic analysis and improvement of a novel solar driven atmospheric water generator. Energy Convers. Manage. 161, 104–111. http://dx.doi.org/10.1016/j.enconman.2018.01.066.

Shourideh, A.H., Bou Ajram, W., Al Lami, J., Haggag, S., Mansouri, A., 2018. A comprehensive study of an atmospheric water generator using Peltier effect. Therm. Sci. Eng. Prog. 6, 14–26. http://dx.doi.org/10.1016/j.tsep.2018.02.015.

Singh, M., Pawar, N.D., Kondaraju, S., Bahga, S.S., 2019. Modeling and simulation of dropwise condensation: a review. J. Indian Inst. Sci. 99 (1), 157–171.

Su, X., et al., 2017. Multi-scale microstructural thermoelectric materials: Transport behavior, non-equilibrium preparation, and applications. Adv. Mater. 29 (20), 1602013. http://dx.doi.org/10.1002/adma.201602013.

Tan, F., Fok, S., 2013. Experimental testing and evaluation of parameters on the extraction of water from air using thermoelectric coolers. J. Test. Eval. 41 (1), 96–103.

Th. Mohammad, A., Mat, S.B., Sulaiman, M.Y., Sopian, K., Al-abidi, A.A., 2013. Survey of liquid desiccant dehumidification system based on integrated vapor compression technology for building applications. Energy Build. 62, 1–14. http://dx.doi.org/10.1016/j.enbuild.2013.03.001.